Journal of Dynamic Behavior of Materials (2024) 10:92–97
https://doi.org/10.1007/s40870-023-00402-w

RESEARCH PAPER

Rationalization of Ring Fragmentation Data via Simple Kinetic Energy Analysis

J. D. Robson[1]

Received: 13 July 2023 / Accepted: 17 November 2023 / Published online: 21 December 2023

Abstract

The available data on fragmentation of alloy rings at high strain rate has been reviewed and analysed with reference to a classical statistical and energetic model. The data have also been compared to a simple calculation based on the specific kinetic energy of the ring. It is shown that fragmentation data for alloys with over a 20 times difference in strength and 7 times difference in density scatter around a single curve when plotted as a function of specific kinetic energy over a wide range of strain rates. A fit to this curve therefore provides an approximate estimate of the expected fragment number for any ductile metal without requiring any detailed knowledge about the constitutive behaviour or defect population. This fit is better than a prediction based on the classical statistical model, and similar to that for the energetic model, which also requires a knowledge of the fragmentation fracture energy. The observation that specific kinetic energy alone can explain much of the difference observed between alloys suggest that the energy in the system is more important that details of the alloy microstructure or properties in controlling the number of fragments for a material that fails by ductile fracture. The fit does not work for a case where one alloy was heat treated to a condition where brittle failure occurred.

Keywords Fragmentation · Mott ring · Metals and alloys

Introduction

The ability to predict natural fragmentation of metals is of critical importance in a range of industrial and military applications. As such, there is a large body of research dedicated to understand the factors and relationships that link the material properties and imposed conditions (e.g. strain rate) to the size and velocity of fragments produced in a natural process. However, this remains a challenging problem, since the natural fragmentation process is stochastic on the macro-scale and occurs very rapidly, making reproducible experiments difficult to perform.

The natural fragmentation problem is simplified by removing the complicating effect of realistic geometries. Given its simplicity, the expanding cylindrical ring is a popular test that produces natural fragmentation. A typical cylindrical ring test consists of a thin walled ($\simeq$ 1mm), short ($\simeq$ 1mm) cylinder of diameter $<$ 30mm [1]. These rings are then expanded at high strain rate, with the force driving the expansion coming from explosives or magnetic induction. The magnetic induction method is preferred to provide a reproducible and consistent expansion velocity. Magnetic methods can produce radial ring expansion velocities up to 300 m s^{-1} [1]. Providing the expansion of the ring can be measured accurately and the driving impulse is well known, a ring expansion test can be used to determine both the high strain rate constitutive behaviour (stress–strain response) and the fragmentation behaviour [1, 3].

The classical model by Mott [4] predicts that there is a characteristic distribution of fragment sizes after high strain rate fracture of a ring. In Mott's analysis, the material property that controls the fragment size distribution is the scatter in the local fracture strains and it is thus a statistical model. Other models for fragmentation consider fragmentation based on the energy required to generate the necessary fractures [1]. Although based on different theory, both approaches can give similar predictions, which are in reasonable agreement with experiment [1].

Grady has reviewed the results of several ring fragmentation studies and compared them to theory [1]. One intriguing plot is presented in this review (Fig. 8.11 [1]) in which

✉ J. D. Robson
joseph.d.robson@manchester.ac.uk

[1] Department of Materials, University of Manchester, Royce Hub Building, Manchester M13 9PL, UK

the number of fragments for two distinctly different alloys collapse onto a single curve when plotted as a function of the expansion kinetic energy. However, as Grady notes, this observation for only two materials from two studies could certainly be fortuitous and warrants further study.

The objective of the present analysis is to perform this further study by compiling data from a wide range of ring fragmentation experiments and investigating whether simple scaling to specific kinetic energy still holds. The ability of such scaling to predict the number of fragments has been compared to that of the statistical and energetic fragmentation models. This in turn can focus efforts to develop better models for natural fragmentation.

Methodology

Fragmentation data have been gathered for a wide range of alloys from previous literature studies of ring expansion. Only data for which specimens conform to the ideal Mott ring geometry, and for which reliable measurements were made of the expansion velocity and final fragment number, were considered. A number of ring expansion studies reported in the literature did not meet all of these requirements and therefore were excluded from the analysis (e.g. [5] in which the number of fragments was not reported or [6] in which only the sum of necks and fractures is reported).

The alloys included, sources of the data, and relevant physical and mechanical properties are shown in Table 1. The fragmentation fracture toughness K_f, a property discussed in detail later, was not reported for Mild Steel ES, Al-6061-O, and AA-5052-O. For the aluminium alloys, it was assumed the same value as for Al-1100-O could be applied, which is not unreasonable given that all these materials are in a soft temper state and have a similar elongation to failure. For Mild Steel ES and AZ31B the values used were the plane strain fracture toughness K_{1c}. It can be seen that the alloys cover a wide range of strengths (a factor 20 difference from weakest to strongest), densities (a factor 7 difference between least and most dense), and elongations to failure (a factor 2 difference between the lowest and highest values). They therefore encompass the range of alloys of practical interest.

Results and Discussion

A plot of the data showing the number of fragments as a function of the radial expansion strain rate imposed in the test is shown in Fig. 1. To produce this plot, the velocity at the point of fragmentation was identified from the literature studies and converted to strain rate based on the ring geometry. The number of fragments was taken directly from each paper. Since there is only one experiment for each condition, it is not possible to determine reliable error bars, However, the considerable scatter in the results that reflects the stochastic nature of the fragmentation process gives an indication of the uncertainty in fragment number for a given strain rate, which is typically around 10% from a mean value (determined by comparing similar conditions).

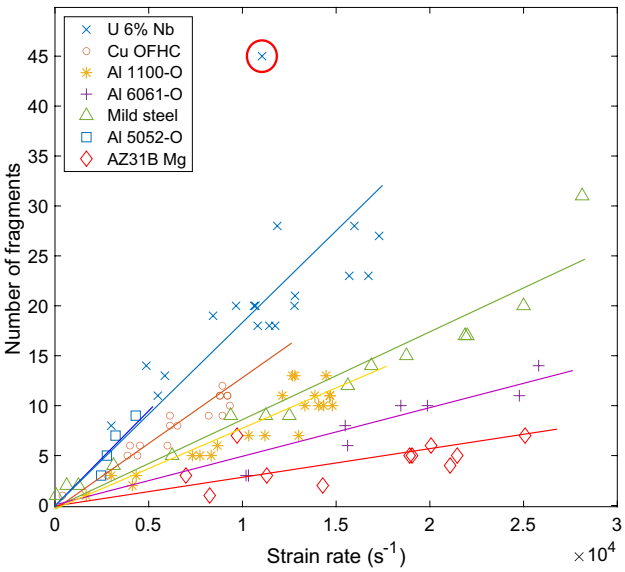

Fig. 1 Measured number of fragments as a function of strain rate for Mott ring data compiled from the literature (see Table 1)

Table 1 Density (ρ) and mechanical properties (yield stress, Y, strain to failure ϵ_f, fragmentation toughness K_f) of alloys for which data has been obtained from listed reference

Alloy	ρ (kg m^{-3})	Y(MPa)	ρ/Y(kg MJ^{-1})	ϵ_f(%)	K_f(MPa m$^{\frac{1}{2}}$)	Reference
U 6 wt% Nb	190,000	730	26	18	60	[7]
Mild Steel ES	7800	250	31	20	140*	[2]
Al-1100-O	2710	35	77	25	60	[8]
Al-6061-O	2710	55	49	20	60	[9]
Cu OFHC	8960	70	128	40	140	[8]
Al-5052-O	2710	100	27	20	60	[10]
Mg-AZ31B	1770	180	10	23	50*	[11]

*For mild steel and magnesium AZ31B, K_f is unknown, so K_{1c} is reported

A number of general observations can be made from this plot. Firstly, the number of fragments increases as the strain rate increases, which is expected from classical fragmentation models [7]. Secondly, there is a systematic difference between the number fragments that becomes apparent as the strain rate increases. The highest number of fragments is produced in the highest density alloy and the lowest number is produced in the lowest density alloy.

There is one data-point for the U–6 wt% Nb alloy that is a clear outlier (circled in red). This point corresponds to a different heat treatment variant of the U–6 wt% Nb alloy, discussed in detail elsewhere [7]. This heat treatment produces a high fraction of brittle α phase, and in this condition the failure of the specimens was observed to occur with very little ductility but instead by cleavage fracture [7]. The number of fragments in this case lies well outside the general trend-line for this alloy in a more ductile state, even accounting for scatter.

Grady [1] demonstrated that by plotting the number of fragments as a function of specific kinetic energy, the data for the Al-1100-O and Cu-OFHC alloys clustered around a single curve. The specific kinetic energy is given by:

$$T = \frac{1}{2}\rho u.^2 \tag{1}$$

where ρ is the alloy density and u the radial expansion velocity.

This analysis is now extended to all the available data from the literature, and the resulting figure is shown in Fig. 2a. The previously noted scatter in the data notwithstanding, this is consistent with Grady's finding [1], showing the results when plotted in this form are scattered approximately around a single curve. At higher specific kinetic energy, a systematic difference is apparent between mild steel and U 6 wt% Nb data, although the highest strain rate measurement, which was for mild steel, lies close the the extrapolation of a best fit line from the U 6 wt% Nb. More data are required in the higher specific kinetic energy regime ($> 1 \times 10^8$J m^{-3}) to draw any clear conclusions about how well this data conforms to a simple kinetic energy fit.

Grady [1] showed the functional form of the best fit line is:

$$N_T = \left(\frac{T}{\tau}\right)^{\frac{1}{2}} \tag{2}$$

where N_T is the number of fragments per length and τ is a fitting parameter. Setting the constant τ to provide the best fit ($\tau = 694$KJ m^{-3}) gives the line shown in Fig. 2a. It can be seen that all the data are scattered around this line, and all points fall within or close to the upper and lower bound lines drawn at $1.5N_T$ and $0.5N_T$.

Since much of the data is clustered at the lower strain rate range, this portion of the graph has been magnified in Fig. 2b. The scatter is large, but the fit of Eq. 2 remains approximately valid over this narrower range. Notably, the systematic difference between different alloys is largely eliminated when plotting the number of fragments as a function of specific kinetic energy.

This simple analysis based only on the kinetic energy can be compared with the other models used to rationalize fragmentation data. As discussed in the introduction, there are

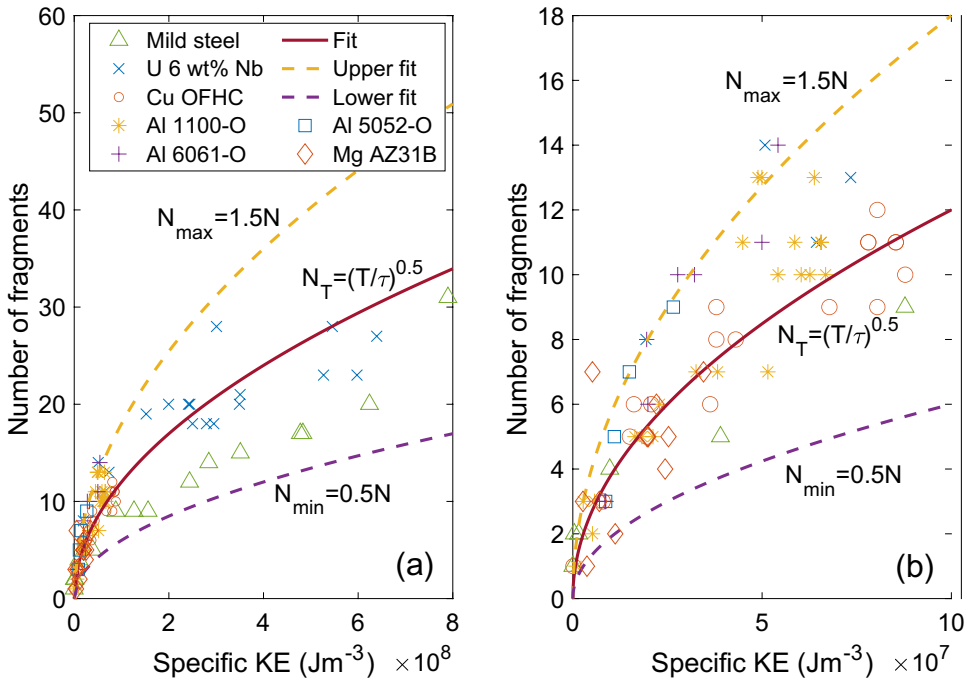

Fig. 2 **a** Measured number of fragments as a function of specific kinetic energy for Mott ring data compiled from the literature (see Table 1), **b** zoomed into the lower strain rate range

two distinct theoretical approaches. The method of Mott [4] is based on the assumption that the number of fragments is controlled by the statistical distribution of fracture strains around the ring. Further details of the Mott model are given elsewhere [4, 7]. The Mott model gives the number of fragments as:

$$N_S = \left(\frac{\rho\dot{\epsilon}^2}{2\pi Y}\frac{n}{\sigma}\right)^{\frac{1}{2}} \tag{3}$$

where Y is the yield stress of the alloy and n/σ are the parameters that define the hazard function (distribution of fracture strains [1, 4]). Since the latter are not known a priori, this equation cannot usually be used to make a forward prediction of the fragment number. However, if it is assumed that the hazard function is identical for all alloys, Eq. 3 can be directly applied and used to predict the total fragment number, which can be compared with a prediction based on the simple kinetic energy approach. Taking the standard deviation in strain-to-fracture at high strain rate as 0.05 (a value shown to be reasonable for copper [1]), the predictions are as shown in Fig. 3a.

It can be seen that this analysis does not represent the underlying trends in the data well. Although the number of fragments predicted in each case is correct to within a factor of 2, the relative number of fragments for each material at a given strain rate is wrong. For example, the U 6 wt% Nb alloy is predicted to produce the fewest fragments, whereas in practice it produces the most. This could be corrected by assuming this alloy has a different distribution of fracture strains, but then the model is not predictive. In the Mott analysis, assuming the distribution of fracture strains is invariant between alloys, the only material parameter controlling the number of fragments is ρ/Y. Values for this ratio are presented in Table 1. The highest density material (U 6 wt% Nb) also has the highest yield strength, so that the ρ/Y ratio is not maximized for this material. Rather, this ratio is greatest for the Cu–OFHC material that has a relatively high density but low strength, which explains why the greatest number of fragments are predicted for this alloy using the statistical model, which is not consistent with observations.

It is also noteworthy that this analysis produces no better prediction of the fragment number than the simple kinetic energy based method. It could be made accurate by tuning the assumed standard deviation in local strain-to-failure at the strain rate of interest for each material separately, but this would require calibration to a large number of experiments. It is therefore not predictive without experimental calibration for each material case.

The second theoretical approach is the energy based theory of Grady [12] and Kipp and Grady [13]. In this model, the energy dissipation associated with growing the fracture and the associated delay time is critical in controlling the fragment size distribution. The material parameter controlling the energy dissipation to grow a fracture is identified as the fragmentation toughness, given the symbol K_f to recognise its relationship to the more well known quasi-static fracture toughness K_c. As with the statistical model, this parameter is not usually known a priori and has to be fitted to data from fragmentation experiments. However, it has been shown that in some cases, K_f and K_{1c} are similar (within a factor of 2) [7], so that in the absence of better data, the quasi-static fracture toughness

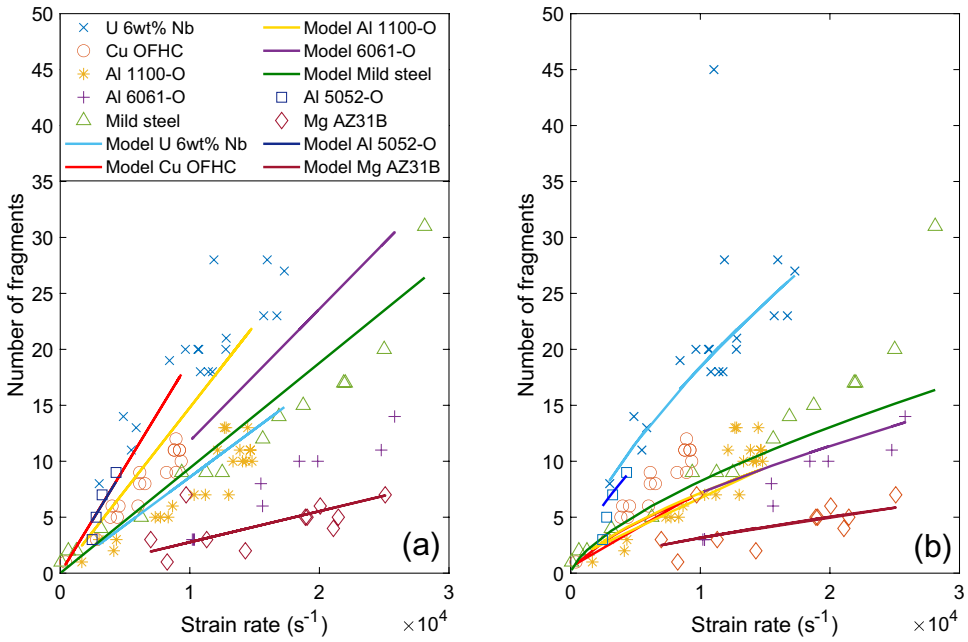

Fig. 3 Measured number of fragments as a function of strain rate with predicted results from **a** the statistically based fragmentation model (lines), and **b** the energy based fragmentation model (lines)

may provide a useful approximation. Data for K_f (or K_{1c} where K_f is unknown) are reported in Table 1.

The energy based model gives the number of fragments per unit length for a given material and strain rate as [7]

$$N_E = \left(\frac{\rho c \dot{\epsilon}}{\sqrt{12} K_f} \right)^{\frac{2}{3}} \quad (4)$$

where c is the velocity of sound in the ring, given by $\sqrt{E/\rho}$ with E being the Young's modulus. Using the data in Table 1, Eq. 4 was applied to calculate the total number of fragments for the alloys of interest in this study, and the results are plotted in Fig. 3b.

It can be seen that this model has given predictions that are in much better agreement with observation than those obtained with the statistical (Mott) model. In particular, the larger number of fragments observed in the U 6 wt% Nb alloy at a given strain rate is correctly captured. Of course, one reason for this better fit is that the critical material parameter (K_f) is different for each alloy, so that the fracture behaviour becomes alloy sensitive. However, even in the case where K_f is approximated by K_{1c} (Mild Steel ES), the agreement remains good, at least until the highest strain rate. Although the fit is clearly better than in the case of the statistical model, it is noteworthy than the maximum error in the number of fragments predicted is still greater than the simple kinetic energy fit. For example, for Cu OFHC, the energy based model underestimates the total number of fragments by a factor of 2 for some strain rates. This fit could of course be improved by refining K_f for that particular material, but this makes a forward prediction for a new material impossible.

It should be noted that both the statistical and energy models are physically based, and seek to explain how the observed number of fragments relates to the underlying controlling mechanisms, whereas no mechanism is inferred from the kinetic energy fit. However, the confirmation of the original observation by Grady [1] that a simple relationship exists between the number of fragments and kinetic energy in the ring suggests that details of the local material properties (flaw distribution, microstructure etc.) are far less important that the overall energy driving the fragmentation process.

Finally, the outlying point for the U 6 wt% Nb alloy may be noted, where the number of fragments observed was far greater than any of the models predict. As mentioned, this point corresponds to material heat treated into a much more brittle state, where low ductility fracture was observed. As the material becomes inherently more brittle, its failure becomes more sensitive to small flaws and the scatter in failure strains in expected to be much larger (of the order of 20% rather than less than 5% [4]). Plastic relaxation at crack tips is more difficult than in a ductile metal, driving high levels of stress concentration. In such cases, it may no longer be reasonable to ignore the local variations within the material. The analysis here therefore appears valid only if there is sufficient ductility to reduce the effect of initial defects so that inertial effects dominate. If the material fails without significant plastic deformation, this analysis will probably underestimate the number of fragments considerably.

Conclusions

The available data in the literature on fragmentation of Mott rings has been compiled for a range of very different alloys, ranging from a strong and high density U 6 wt% Nb alloy to a weak, low density aluminium alloy (1100–O). The data have been used to confirm an initial suggestion by Grady [1] based on a much more limited dataset; namely that the number of fragments for these disparate alloys collapses onto a single curve of best fit when plotted as a function of the kinetic energy of the ring. The following conclusions may be drawn from this work.

1. Although the experimental data have a high degree of scatter, a simple fit of fragment number to kinetic energy provides a remarkably good representation. The best fit relation scales with the square root of the kinetic energy.
2. The simple kinetic energy analysis provides a comparable fit to the fragmentation data than a classical physical analysis based on either the statistical or energetic fragmentation theory, at least for the case where accurate material data are not available for the physical models.
3. One datapoint does not fit any of the models, and this corresponds to the U 6 wt% Nb alloy heat treated to a more brittle condition. This implies the current analysis is only valid in the case of ductile metals, where there is significant plasticity associated with failure.

Acknowledgements The author acknowledges the support of DSTL/RAEng Chair in Alloys for Extreme Environments and is grateful to staff at DSTL for valuable discussions, in particular Prof Daniel Pope, Joseph Cordell, and Daniel Armstrong. The EPSRC are thanked for financial support via LightFORM (EP/R001715/1).

Data Availability The data required to reproduce these findings are available from the LightFORM Zenodo repository https://zenodo.org/communities/lightform/.

Declarations

Competing interests The author has no competing interests. This work was funded by the DSTL/RAEng Chair in Alloys for Extreme Environments and EPSRC via the LightFORM programme grant (EP/R001715/1).

References

1. Grady D (2007) Fragmentation of rings and shells: the Legacy of NF Mott. Springer
2. Rusinek A, Zaera R (2007) Finite element simulation of steel ring fragmentation under radial expansion. Int J Impact Eng 34(4):799–822
3. Warnes R, Duffey T, Karpp R, Carden A (1981) An improved technique for determining dynamic material properties using the expanding ring. Shock Waves High-Strain-Rate Phenom Metals Concepts Appl. https://doi.org/10.1007/978-1-4613-3219-0_2
4. Mott NF (1947) Fragmentation of shell cases. Proc R Soc London Ser A: Math Phys Sci 189(1018):300–308
5. Janiszewski J (2012) Ductility of selected metals under electromagnetic ring test loading conditions. Int J Solids Struct 49(7–8):1001–1008
6. Kahana E, Ben-Artzy A, Sadot O, Shneck RZ (2015) Microstructural evolution of AZ31 magnesium alloy after high strain rate expanding rings tests. Mater Sci Eng, A 641:274–280
7. Grady D, Olsen M (2003) A statistics and energy based theory of dynamic fragmentation. Int J Impact Eng 29(1–10):293–306
8. Grady D, Benson D (1983) Fragmentation of metal rings by electromagnetic loading. Exp Mech 23(4):393–400
9. Zhang H, Ravi-Chandar K (2007) On the dynamics of necking and fragmentation - I. real-time and post-mortem observations in al 6061-O. Int J Fract 142(3–4):183–217
10. Ma H, Mao W, Su H, Zhu H, Cui X, Huang L, Li J, Wu M (2021) Rate-related study on mechanical properties and fracture characteristics in aluminium alloy via electromagnetic ring expansion test. Int J Mech Sci 209:106712
11. Cliche N, Ravi-Chandar K (2018) Dynamic strain localization in magnesium alloy AZ31B-O. Mech Mater 116:189–201
12. Grady DE (1982) Local inertial effects in dynamic fragmentation. J Appl Phys 53(1):322–325
13. Kipp M, Grady D (1985) Dynamic fracture growth and interaction in one dimension. J Mech Phys Solids 33(4):399–415